

Activation of the JAK1/STAT1 signaling pathway is associated with peroxiredoxin 6 expression levels in human epididymis epithelial cells

Hui Shi^{1, #}, Xiaoyu Liu^{2, #}, Yanwei Wang³, Haiyan Wang³, Bochen Pan^{2, *}, Jianyuan Li^{4, *}

¹College of Life Science, Yantai University, Yantai, Shandong Province, PR China

²Center of Reproductive Medicine, Shengjing Hospital of China Medical University, Shenyang, Liaoning Province, PR China

³Qingdao Medical College Affiliated Hospital of Yantai Yuhuangding Hospital, Yantai, Shandong Province, PR China

⁴Key Laboratory of Male Reproductive Health, National Health and Family Planning Commission, Beijing, PR China

#These authors contributed equally to this work.

Abstract

Introduction. Peroxiredoxin 6 (Prdx6) is widely expressed in mammalian tissues. Our previous study demonstrated that Prdx6 was expressed in human epididymis, present in human seminal fluid, and in spermatozoa. The protective role of Prdx6 in maintaining the viability and DNA integrity of human spermatozoa was also detected. Here, we demonstrate the potential role and mechanism of Prdx6 in human epididymis epithelial cells (HEECs).

Material and methods. Western blotting was used to measure expression levels of key proteins in the Janus kinase/signal transducer and activator of transcription (JAK/STAT) signaling pathway. The malonaldehyde (MDA) levels and antioxidant capacity in HEECs were detected with the commercial kits. Digital gene expression analysis (DGE) was used to identify gene expression patterns in control and Prdx6-interference HEECs. Reverse transcriptase-polymerase chain reaction (RT-PCR) was used to validate the DGE findings.

Results. Compared to control HEECs, the expression levels of JAK1, STAT1, phosphorylated JAK1 and STAT1 were significantly increased, while the expression level of SOCS3 was significantly decreased in Prdx6-interference HEECs. The MDA level and total antioxidant capacity in Prdx6-interference HEECs were significantly increased and decreased compared to that of control, respectively. DGE analysis identified 589 up-regulated and 314 down-regulated genes (including *Prdx6*) in Prdx6-interference HEECs. Thirteen significantly different pathways were identified between the two groups, with the majority of genes belonging to the CCL, CXCL, IL, and IFIT family of proteins and were related to immunity. In particular, the expression levels of *IL6*, *IL6ST*, and eighteen IFN-related genes were significantly increased in Prdx6-interference HEECs compared to control HEECs.

Conclusions. We found that reduced Prdx6 expression induced higher ROS levels in HEECs, which resulted in the activation of the *IL-6* receptor and *IFN γ* expression to induce the JAK1/STAT1 signaling pathway. (*Folia Histochemica et Cytobiologica* 2022, Vol. 60, No. 3, 226–236)

Keywords: Prdx6; human epididymis epithelial cells; RNAi; DGE; JAK1; STAT1

*Corresponding authors:

Jianyuan Li and Bochen Pan

Yantai University, No. 30 Qingquan Road, Yantai, 264005,
P. R. China

phone: 86-535-6902638; fax: 86-535-6902638

e-mails: sdscli@126.com; panbochen@cmu.edu.cn;

lijianyuan2021@126.com

Introduction

Peroxiredoxins (Prdxs) are antioxidant enzymes composed of six family members (Prdx1–6) [1]. Prdx1–5 contains 2-Cys, while Prdx6 contains only 1-Cys [2].

The primary function of Prdxs is to prevent oxidative damage induced by reactive oxygen species (ROS) [3]. The relationship between Prdxs, inflammation, and immunity has been widely reported. Prdx1 act as an immunomodulator in macrophages and endothelial cells [4] and has been associated with the occurrence of atherosclerosis and rheumatoid arthritis [5]. Moon *et al.* [6] demonstrated the inhibitory function of Prdx2 in immune cell responsiveness, while Szabó-Taylor *et al.* [7] demonstrated the role of Prdx2 in chronic inflammation and the relationship between Prdx2 and the occurrence of rheumatoid arthritis. Prdx3 is the only member that lacks an immunomodulatory function, and its deficiency has been shown to increase abnormal lipid accumulation in adipose tissue [8]. Prdx4 inhibits inflammation induced by oxidative stress in various tissues, such as breast, prostate, ovary, colon, rectum, lung, cardio- and cerebrovascular system [9], and its molecular mechanism may be *via* the regulation of NF- κ B, which is an important pro-inflammatory transcription factor [10]. The expression of Prdx4 has also been shown to be associated with rheumatoid arthritis [11]. Prdx5 regulates inflammatory processes through the thioredoxin (Trx) system, which plays a critical role in cell activities [12]. While Prdx6 has been shown to be involved in regulating cell proliferation, apoptosis, embryonic development, lipid metabolism, immune response, and osteogenic differentiation [13–16]. Furthermore, Prdx6 has been shown to activate the NF- κ B/AP-1 and JNK pathways, which is necessary for the development of rheumatoid arthritis [17].

There are four Janus kinases (JAKs) and seven signal transducer and activator proteins (STATs) found in mammals. The JAK/STAT signaling pathway is triggered by:

1. the binding of extracellular ligands to cell surface receptors to activate receptor-associated JAKs;
2. JAKs phosphorylate and activate cytoplasmic STAT dimers;
3. phosphorylated STAT translocates to the nucleus and regulates target gene expression [18].

The JAK/STAT pathway is a conserved signaling system, which is well known to function in immunity, regulation of homeostatic processes in germline and somatic stem cells, and regenerative processes in the gonads, intestine and appendages [19]. The suppressor of cytokine signaling (SOCS) proteins provides selective negative feedback to STAT activation to

prevent over-stimulation of the immune system. Of the eight members, only SOCS1 and SOCS3 have been well studied. SOCS1 and SOCS3 have been shown to inhibit the components of the JAK/STAT signaling pathway in a highly cell-type-specific manner [20, 21]. Fernandez *et al.* [22] demonstrated that Prdx6 functioned in antioxidant defense in human spermatozoa. Mammalian epididymis generates a complex mixture of intraluminal fluids required for post-testicular maturation and storage of spermatozoa. This provides in the epididymis the environment for mammalian spermatozoa to develop motility and fertilization ability [23, 24]. However, the function of Prdx6 in epididymis remains to be studied.

Based on the role of Prdx6 in the immune response and the regulatory role of the JAK/STAT signaling pathway during the immune responses [13, 15, 17], we investigated the possible relationship between Prdx6 and the JAK/STAT signaling pathway in human epididymis epithelial cells (HEECs).

Materials and methods

Culturing human epididymis epithelial cells. HEECs, which have been passaged 27 times, were kindly provided by Daniel G. Cyr (INRS-Institut Armand Frappier, University of Quebec, Laval, Quebec, Canada) [25]. HEECs were cultured in DMEM/HAM F12 media with penicillin (50 U/mL), streptomycin (50 lg/mL), L-glutamine (2 mM), insulin (10 lg/mL), transferrin (10 lg/mL of), hydrocortisone (80 ng/mL), testosterone (5 nM), epidermal growth factor (10 ng/mL), cAMP (10 ng/mL), sodium selenium (2 ng/mL), tocopherol (200 ng/mL), retinol (200 ng/mL), and 10% fetal bovine serum (FBS) (Sigma-Aldrich, Burlington, MA, USA). Cells were seeded in culture plates coated with collagen IV (BD Biosciences, Mississauga, Canada) and incubated in a humidified chamber at 32°C with 5% CO₂. The cells, used for the subsequent experiments, were resuscitated and subcultured for 2 times. The cell type was confirmed with RT-PCR, which was used to detect the epididymal principal cell markers (NPC2, DCXR, CD52, SLC9A3). The state of cell growth was detected with methylthiazolyldiphenyl-tetrazolium bromide (MTT) assay and Trypan blue staining.

Construction of the Prdx6 shRNA expression plasmid. The short hairpin RNA (shRNA) sequences targeting the mRNA of the human Prdx6 gene (Gens ID: 9588) were designed using the online tool (http://www.genesil.com/siRNA_design.asp) [26] (Table 1). The Prdx6 shRNA sequences were then inserted into the endonuclease loci of *Bam*HI and *Hind* III in the pGenesil-1 vector (Wuhan GeneSil Biotechnology, Wuhan, China). The shRNA sequences were specific and did not target mRNA sequences of other known human genes.

Plasmid transfection. The HEECs at 80% confluency were transfected with the Prdx6 shRNA expressing construct using the FuGENE HD Transfection Reagent (Roche, Mannheim, Ger-

Table 1. Target sequence of interference for human Prdx6

shRNA name	Position on CDS	Target sequence	GC content (%)
si Prdx6	667	AGCTGGCACCAGAATTGCCAAGAG	52
irrelevant (control)		AGCTAGCACTAGAATCTGCCGAGAG	52

many). In addition, the HEECs transfected with non-targeting shRNA constructs were used as the control.

Protein extractions and Western blot analysis. Total proteins were extracted from 48 h post-transfected HEECs using RIPA lysis buffer (P0013B, Beyotime Biotechnology, China) supplemented with PMSF (ST506, Beyotime Biotechnology) and protease phosphatase inhibitors (P1050, Beyotime Biotechnology). Total proteins were then separated on a 10% (w/v) SDS-PAGE for JAK1 and STAT1 detection and 12% (w/v) SDS-PAGE for SOCS3 and GAPDH detection. After electrophoresis, transferred and blocked membrane, the membrane was incubated with primary antibodies overnight at 4°C. The concentrations of antibody used in the present study were as follows: anti-JAK1 antibody (ab133666, Abcam, UK) was 0.17 µg/mL; anti-JAK1 (phospho Y1022 + Y1023) (ab138005, Abcam) was 0.22 µg/mL; anti-STAT1 (ab47425, Abcam) was 2 µg/mL; anti-STAT1 (phospho Y701) (ab29045, Abcam) was 2 µg/mL; anti-SOCS3 (ab16030, Abcam) was 1 µg/mL; and anti-GAPDH (ab181602, Abcam) was 0.5 µg/mL. After incubation, the membranes were washed with PBS-Tween (1000:1) and then incubated with the relevant HRP-labeled secondary antibody for 2 h at room temperature. X-ray film (Bio-Rad, Hercules, CA, USA) was used for chemiluminescent detection of target proteins. Experiments were performed in triplicates.

Detection of malonaldehyde levels and total antioxidant capacity of HEECs. The malonaldehyde (MDA) levels and total antioxidant capacity in HEECs of control and Prdx6-interference were detected with commercial kits (S0131S, Beyotime Biotechnology and A015-2-1, Nanjing Jiancheng Bioengineering Institute, respectively) according to the manufacturers' protocol.

Sample preparation and RNA isolation. Total RNA was extracted from 48 h post-transfected cells using TRIZOL (Invitrogen, Carlsbad, CA, USA). RNA quality was measured using ultraviolet spectrophotometry and denaturing agarose gel electrophoresis.

DGE library preparation and sequencing. Library preparation and sequencing were performed by BGI using the Illumina Gene Expression Sample Prep Kit and Solexa Sequencing Chip (flowcell) on the Illumina Cluster Station and Illumina HiSeq™ 2000 System.

Data transformation and Gene annotation. Raw solexa sequences were transformed using the following steps:

1. removal of the 3' adaptor sequence, empty reads, and low-quality tags;
2. selection of 21st read length tags;
3. removal of single copy tags;

4. generation of Clean Tags. After quality assessment, the clean tags were used to generate alignment statistics between the Prdx6-interference and control cells.

All clean tags were mapped to the reference sequence and only 1bp mismatch was considered during alignment. The number of unambiguous clean tags for each gene was calculated and then normalized to TPM (number of transcripts per million clean tags) [27, 28].

Differently expressed genes. Differently expressed genes between the two groups were determined using the Audic-Claverie method [29]. The threshold used to determine significant differences in gene expression was based on False Discovery Rate (FDR) ≤ 0.001 and the absolute value of log₂Ratio ≥ 1, as described in Benjamini, Yekutieli [30].

Gene Ontology functional enrichment and Genomes pathway enrichment analysis. Gene Ontology (GO) functional enrichment and Genomes (KEGG) pathway enrichment analysis were performed to uncover the biological function and metabolic pathways of the differently expressed genes, respectively. Gene Ontology analysis was performed based on the methods used by Ye *et al.* [31]. Significantly enriched metabolic and signal transduction pathways were identified using the KEGG public database [32].

RT-PCR. Total RNA was extracted using TRIZOL (Invitrogen, Carlsbad, CA, USA) based on the manufacturer's instructions. Gene-specific primer sequences and PCR conditions are shown in Table 2. The PCR-amplified products were run and analyzed using a 1.5% (w/v) agarose gel.

Results

The expression level of Prdx6 after Prdx6 shRNA transfection

The expression levels of *Prdx6* in cells transfected with Prdx6 shRNA plasmid were 52.7% lower compared to control cells transfected with non-targeting shRNA plasmid (Fig. 1A). This confirmed that our shRNA sequence targeting Prdx6 was effective in knocking down *Prdx6* expression.

The Malondialdehyde level and total antioxidant capacity of HEECs

The MDA level in Prdx6-interference HEECs was significantly increased compared to that of control. The total antioxidant capacity, meanwhile, showed the opposite trend (Fig. 1C, D).

Table 2. The sequences and melting temperature of primers

Gene name	Primer(5'–3')	Tm (°C)
<i>GAPDH</i>	F: AACGGATTGGTCGTATTG; R: GGAAGATGGTGATGGGATT	51.5
<i>ICAM1</i>	F: TAGCAGCCGCAGTCATAAT; R: AGAAAGTTGGGCAGGGAG	53
<i>IL6</i>	F: GTCCAGTTGCCTTCTCCC; R: GCCTCTTGCTGCTTCA	53.7
<i>IDO1</i>	F: CTGGAAGTGCCTCCTATT; R: ATGCGAAGAACACTGAAA	49.5
<i>TLR4</i>	F: GACCTGTCCCTGAACCCTA; R: AAATGTTGCCATCCGAAA	49
<i>EDN2</i>	F: ACTTGGACATCATCTGGGTG; R: GAGGCTCTTGACTGTGGAAA	57
<i>BIRC3</i>	F: TGGTGGTATGTGCCTGTA; R: TGGAAAGAGTCTGGGAGT	48.1
<i>TSNAX</i>	F: TTAATATCGTGCCAAGCC; R: CCTCGTGATCTGCCTACC	49
<i>MTOR</i>	F: AAAACCTCGTCACATTACCC; R: CAGCGAGTCTTGTCTATTCC	54.1
<i>CCL2</i>	F: TGCTTCCCTTTCCTACTT; R: TGGATGTTTCTGGGTTAGT	51.1
<i>CCL4</i>	F: TCGCAACTTTGTGGTAGA; R: TTCAGTTCAGGTCATACAC	50.5
<i>CCL5</i>	F: CCCTCGCTGTCATCCTCA; R: CCCTCGCTGTCATCCTCA	56.1
<i>BYSL</i>	F: GGGAGCAAATCCTCTACG; R: CACAGCACAGGCAGTTCA	54
<i>FOSL</i>	F: ATTCAAATCCGCCCTGTC; R: ATGCGTCGTTTCTCCTCC	53.1
<i>SHC1</i>	F: GGGGAGGAGTAACCTGAAA; R: TGGCAACATAGGCGACAT	53.8
<i>ASNS</i>	F: CTTCTGAGGGAACTCTATT; R: AGCTGACTTGTAAGTGGGT	49.1
<i>GAMT</i>	F: CCTGCCTGACGGTCACTT; R: CCTCCATACGGATGTTCTCC	56.5
<i>UCP2</i>	F: GCTGGAGGTGGTCGGAGAT; R: GGAGGCGATGACAGTGGT	55.4
<i>PPIA</i>	F: TTTGCAGACAAGTCCCA; R: TTGCCATCCAACCACTCA	52.4
<i>MMP14</i>	F: CATCATTGAGGTGGACGAG; R: CATCATTGAGGTGGACGAG	56.9
<i>WNT7B</i>	F: TAGACACCCTCTGTTTCCTTTC; R: TAGACACCCTCTGTTTCCTTTC	56
<i>SPATA20</i>	F: AGTCACCATACCTCCTACAACA; R: TCCTCACGGTCTACCTTAC	53.7
<i>Prdx6</i>	F: AATTTGCCAAGAGGAATG; R: GTGGTAGCTGGGTAGAGG	50.8

Tm — the melting temperature

The JAK/STAT signaling is activated in HEECs transfected with Prdx6 shRNA plasmid

Compared to control HEECs, the protein expression levels of JAK1 and STAT1 were significantly increased in Prdx6-interference group. In addition, the protein expression level of SOCS3 was significantly reduced in HEECs transfected with Prdx6 shRNA plasmid (Fig. 2A, B).

Sequencing quality

The distribution patterns of total and distinct tags were similar between Prdx6-interference and control HEECs. This suggested the absence of bias in the construction of the two libraries (Fig. 3). Tags with copy numbers (showed in the square brackets) > 100 were dominant for both control and Prdx6-interference HEECs, while the majority of distinct tags had copy numbers < 5 (Fig. 3). This indicated that low mRNA levels were more significant.

Differently expressed genes

There were 903 differently expressed genes between the control and Prdx6-interference HEECs. Compared to the control cell, 589 genes were up-regulated and 314 were down-regulated (including Prdx6) in Prdx6-interference group (Fig. 1B).

Functional annotation of DGEs

DGEs were categorized into biological processes, molecular function, and cellular components (Fig. 4). The relevant biological processes were cellular protein metabolic process, metabolic process, multi-organism process, response to other organisms, and response to a biotic stimulus. The relevant molecular function was cytokine activity. The relevant cellular components contained ribosomal subunit, ribosome, cytoplasmic part, cytoplasm, organelle part, intracellular organelle part, membrane-bounded organelle, intracellular membrane-bounded organelle, organelle, intracellular organelle, intracellular part, and intracellular.

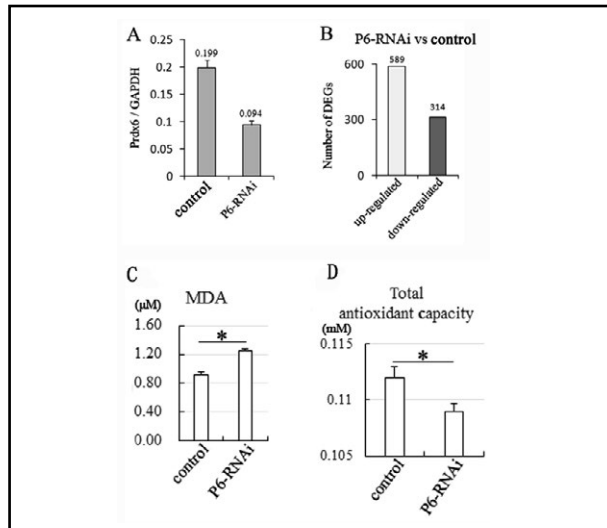


Figure 1. Expression levels of *Prdx6* (A), number of the differently expressed genes (B), the MDA levels (C), and total antioxidant capacity (D) of human epididymis epithelial cells (HEECs). A. Expression levels of *Prdx6* in Prdx6-interference HEECs were reduced by 52.7% compared to control HEECs. B. Compared to control HEECs, there were 589 up-regulated genes and 314 down-regulated genes (including *Prdx6*) in Prdx6-interference HEECs. C. The MDA level in Prdx6-interference HEECs was significantly increased compared to that of control. D. The total antioxidant capacity, meanwhile, showed the opposite trend. P6-RNAi represented Prdx6-interference HEECs. * $P < 0.05$.

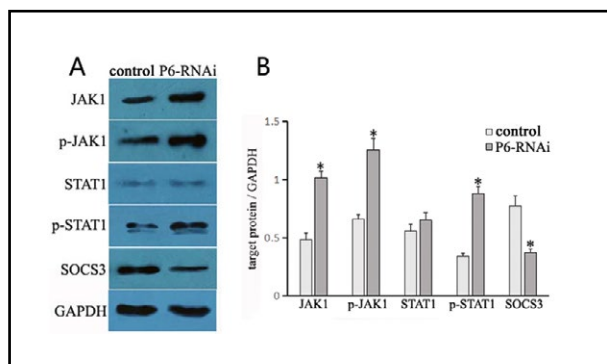


Figure 2. Western blot analysis of JAK1, STAT1, and SOCS3 expression levels (A) and gray degree analysis (B). Compared to control HEECs, the expression levels of JAK1, phosphorylated JAK1, STAT1, and phosphorylated STAT1 were significantly increased, while expression levels of SOCS3 were significantly reduced in Prdx6-interference HEECs. P6-RNAi represented Prdx6-interference HEECs. * $P < 0.05$.

Pathway analysis of DGEs

There were 13 significantly different pathways between Prdx6-interference and control HEECs. We further annotated the genes in the 13 pathways using Wikipedia (https://en.wikipedia.org/wiki/Main_Page). The total number of related genes in the significantly different pathways were 80, of which, 44 genes belonged to the CCL, CXCL, IL, and IFIT family of genes, which were associated with immunity. The

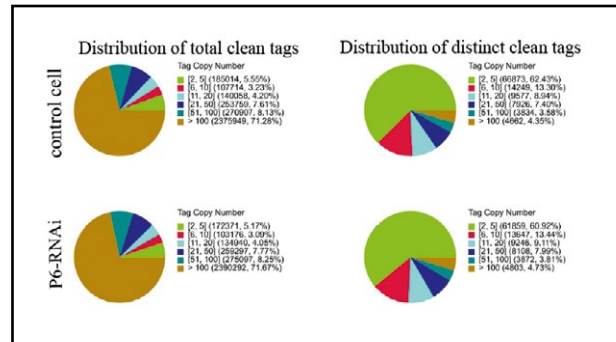


Figure 3. Evaluation of Sequencing Quality. The distribution patterns of total and distinct tags were similar between Prdx6-interference and control HEECs. Tags with copy numbers > 100 were dominant in both control and Prdx6-interference HEECs, while the majority of distinct tags had copy numbers < 5. P6-RNAi represented Prdx6-interference HEECs. The numbers in square brackets represented the tag copy number.

other genes were related to cell growth, ubiquitination, metabolism, ribosomal proteins, and apoptosis-related proteins.

RT-PCR

Eleven up-regulated and ten down-regulated genes were randomly selected for RT-PCR validation. Basically, consistency was observed between RT-PCR and DGE results (Fig. 5).

The expression levels of JAKs, STATs, and SOCSs

Compared to control cells, the mRNA expression levels of JAK1 and STAT1 were significantly increased in Prdx6-interference HEECs. Meanwhile, the mRNA expression level of SOCS3 was significantly reduced in Prdx6-interference HEECs (Table 3).

The expressions of IL-6 receptor family and genes related to IFN γ

Compared to control cells, the expression levels of *IL-6*, *IL6ST*, and downstream genes (*i.e.*, *PIM-3*, and cytokines) were significantly increased in Prdx6-interference HEECs (Table 4).

Although differences in expression levels of *IFN γ* and *IFN γ* receptors were not observed between the control and Prdx6-interference HEECs, the majority of *IFN γ* -related genes (*IFRD1*, *IRF9*, *IF16*, *IF127*, *MX1*, *IF144*, *IF144L*, *IFIT1*, *IFIT3*, *IFITM1*, *IFIT2*, *IFIH1*, *IFIT5*, *IFI30*, *IFITM3*, *GBP1*, *IFI16*, *IRF7*) showed significantly higher expression (Table 5). Furthermore, the expression levels of downstream genes of *IFN γ* signaling (*OAS1*, *OAS2*, *OAS3*, *OASL*, *HLA-A*) were significantly higher in Prdx6-interference HEECs (Table 5). The likely signaling pathways are shown in Fig. 6.

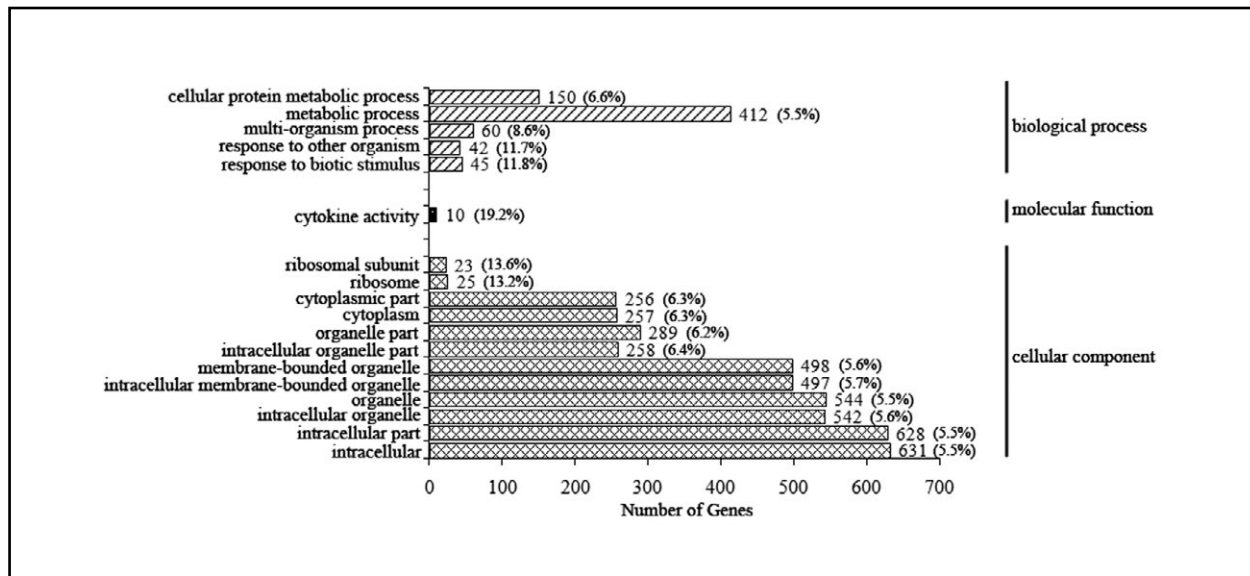


Figure 4. GO functional classification of the DGEs. Y-axis represents GO terms. All GO terms were grouped based on biological process, molecular function, and cellular component. The numbers in the bars represent DGEs annotated for biological process, molecular function, and cellular component. The percentage in the round brackets represent DGEs with relative annotation/all genes with relative annotation.

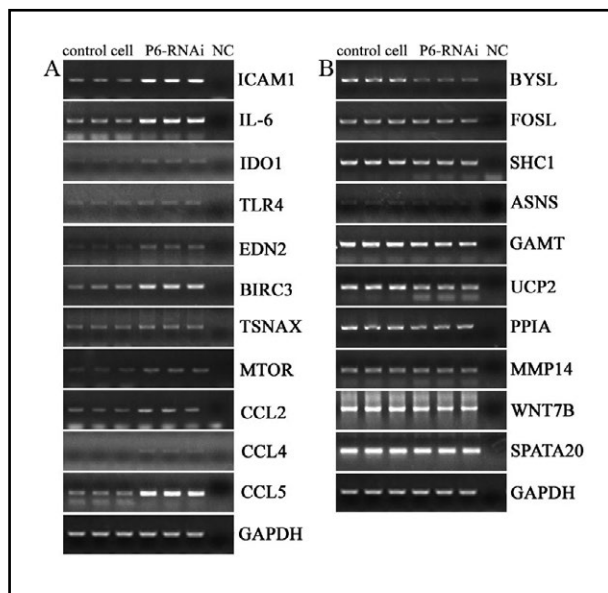


Figure 5. Differently expressed genes measured by RT-PCR. Genes with different expression levels were generally consistent between RT-PCR and DGE profiles. P6-RNAi represented Prdx6-interference HEECs.

Discussion

Prdxs play an important role in reducing several cellular peroxide substrates, such as ROS [13]. Leong *et al.* [33] described the immunomodulatory effects of ROS, which act as second messengers to participate in lymphocyte activation and as a third signal in T cell activation. Hence, we focused here on the relationship between Prdx6 and the expression of immunological-

ly-related signaling molecules in HEECs. Multiple developmental and immunological processes are regulated by the JAK/STAT signaling pathway [34]. In *Drosophila* [19], mice [35], and zebrafish [36], the JAK/STAT pathway is mainly involved in the process of cell proliferation and tissue regeneration. In humans, besides the regulation of regenerative processes in the gonads, intestine and appendages, the JAK/STAT signaling pathway is reported to be related to immune and inflammatory diseases [19]. Yun *et al.* [15] reported that Prdx6 promoted lung tumor development *via* its mediated and CCL5-associated activation of the JAK2/STAT3 pathway in mice. In the present study, we showed that targeted knockdown of Prdx6 significantly increased expression levels of JAK1 and STAT1 in HEECs. Meanwhile, the significantly decreased expression levels of SOCS3, which provides selective negative feedback to the JAK/STAT signaling pathway, was also detected. These results demonstrated that the JAK1/STAT1 pathway was activated along with the knockdown of Prdx6 in HEECs. Baker *et al.* [20] showed that SOCS inhibited the components of the JAK/STAT signaling pathway in a highly cell-type-specific manner. We speculated that there was also cell specificity as to which member Prdx6 was regulated to activate the JAK/STAT pathway.

To validate our results, we analyzed the differential gene expression profiles between Prdx6-interference and control HEECs. Our DGE results showed that expression levels of IL-6, IL6ST, and their downstream targets, *i.e.*, PIM3 and various cytokines, were signifi-

Table 3. The expressions of *JAKs* and *STATs*

Gene symbol	Log ₂ Ratio (Prdx6-interference/ control)	P value	FDR	Significant difference
<i>JAK1</i>	1.34	8.28226E-14	2.6014E-12	*
<i>JAK2</i>	1.35	0.01359128	0.045822224	–
<i>JAK3</i>	–1.94	0.001423868	0.006742904	–
<i>JAKMIP3</i>	–5.906890596	0.2498	0.419522358	–
<i>STAT1</i>	1.02	2.1736E-12	4.39471E-11	*
<i>STAT2</i>	1.12	0.1156098	0.245160301	–
<i>STAT3</i>	–0.09	0.728464	0.827680221	–
<i>STAT4</i>	–0.42	0.725936	0.828291933	–
<i>STAT5A</i>	1.19	0.0641106	0.154290407	–
<i>STAT5B</i>	–0.45	0.0708682	0.166866442	–
<i>STAT6</i>	0.83	0.00974278	0.03466438	–
<i>SOCS1</i>	0.485426827	0.58175	0.720043576	–
<i>SOCS2</i>	–0.599324599	0.00657522	0.0251786	–
<i>SOCS3</i>	–1.605721061	7.16074E-07	6.9378E-06	*
<i>SOCS4</i>	0.426804556	0.0877092	0.197829067	–
<i>SOCS5</i>	–0.237136417	0.419994	0.576760444	–
<i>SOCS6</i>	0.358265781	0.207484	0.370426821	–
<i>SOCS7</i>	0.502753645	0.0282318	0.08299928	–

P value — indicates the probability that a gene is expressed equally between two samples; FDR — false discovery rate; * represents a significant difference between Prdx6-interference and control cell groups; – represents no significant difference between Prdx6-interference and control cell groups.

Table 4. The significantly different expression genes related with IL-6

Gene symbol	log ₂ Ratio (Prdx6-interference/ control)	P value	FDR	Description
<i>IL-6</i>	3.08	8.82E-07	8.43333E-06	Interleukin-6 precursor
<i>IL6ST</i>	1.21	1.86E-13	5.11834E-12	Interleukin-6 receptor subunit beta isoform 3 precursor
<i>PIM-3</i>	1.61	1.94E-05	0.000148023	Threonine-protein kinase pim-3
<i>CXCL10</i>	8.71	6.13E-05	0.000417574	C-X-C motif chemokine 10 precursor
<i>CXCL11</i>	9.91	2.35E-10	3.66318E-09	C-X-C motif chemokine 11 precursor
<i>CCL20</i>	9.23	9.59E-07	9.10857E-06	C-C motif chemokine 20 isoform 1
<i>CCL2</i>	3.17	6.55E-13	1.49744E-11	C-C motif chemokine 2 precursor
<i>CXCL3</i>	2.93	3.17E-09	4.2176E-08	C-X-C motif chemokine 3
<i>CCL4</i>	9.43	1.20E-07	1.30567E-06	C-C motif chemokine 4 isoform 1 precursor
<i>CXCL1</i>	2.99	1.27E-13	3.75194E-12	Growth-regulated alpha protein precursor
<i>CXCL2</i>	2.92	1.03E-11	1.87682E-10	C-X-C motif chemokine 2
<i>CCL5</i>	4.01	1.67E-09	2.33772E-08	Beta-chemokine RANTES precursor
<i>IL8</i>	2.48	1.25E-13	3.70921E-12	Interleukin 8
<i>IL1A</i>	2.81	5.69E-05	0.000390146	Interleukin-1 alpha proprotein
<i>IL17RA</i>	1.32	2.44E-09	3.31192E-08	Interleukin-17 receptor A precursor
<i>IL15</i>	1.24	1.26E-06	1.177E-05	Interleukin-15 isoform 1 preproprotein
<i>IL1I1</i>	2.43	9.42E-05	0.00061488	L-amino-acid oxidase isoform 2

Table 5. The significantly different expression genes related with IFN γ

Gene symbol	log ₂ Ratio (Prdx6-interference/ control)	P value	FDR	Description
<i>IFRD1</i>	1.04	4.20E-07	4.21025E-06	Interferon-related developmental regulator 1 isoform 1
<i>IRF9</i>	1.03	3.05E-11	5.25108E-10	Interferon regulatory factor 9
<i>IFI6</i>	5.39	0	0	Interferon alpha-inducible protein 6 isoform a
<i>IFI27</i>	5.07	1.03E-11	1.87935E-10	Interferon alpha-inducible protein 27, mitochondrial isoform 2
<i>MX1</i>	4.46	4.59E-05	0.000319052	Interferon-induced GTP-binding protein Mx1
<i>IFI44</i>	4.31	4.65E-10	6.97675E-09	Interferon-induced protein 44
<i>IFI44L</i>	4.29	8.82E-07	8.41545E-06	Interferon-induced protein 44-like
<i>IFIT1</i>	3.93	2.78E-13	7.12675E-12	Interferon-induced protein with tetratricopeptide repeats 1 isoform 2
<i>IFIT3</i>	3.92	5.00E-14	1.68269E-12	Interferon-induced protein with tetratricopeptide repeats 3
<i>IFITM1</i>	3.29	2.20E-14	7.7721E-13	Interferon-induced transmembrane protein 1
<i>IFIT2</i>	2.81	0	0	Interferon-induced protein with tetratricopeptide repeats 2
<i>IFIH1</i>	2.81	7.48E-08	8.41713E-07	Interferon-induced helicase C domain-containing protein 1
<i>IFIT5</i>	1.64	2.53E-14	8.87993E-13	Interferon-induced protein with tetratricopeptide repeats 5
<i>IFI30</i>	1.56	1.50E-05	0.00011708	Gamma-interferon-inducible protein precursor
<i>IFITM3</i>	1.46	8.88E-14	2.75131E-12	Interferon-induced transmembrane protein 3
<i>GBP1</i>	1.4	6.02E-07	5.90443E-06	interferon-induced guanylate-binding protein 1
<i>IFI16</i>	1.22	8.69E-10	1.26281E-08	Interferon, gamma-inducible protein 16 variant
<i>IRF7</i>	1.17	2.98E-12	5.89395E-11	Interferon regulatory factor 7 isoform d
<i>OAS1</i>	3.85	2.76E-05	0.000203764	2'-5'-oligoadenylate synthase 1 isoform 3
<i>OAS2</i>	11.17	4.44E-16	1.80117E-14	2'-5'-oligoadenylate synthase 2 isoform 3
<i>OAS3</i>	3.71	7.48E-08	8.42414E-07	2'-5'-oligoadenylate synthase 3
<i>OASL</i>	1.71	0	0	59 kDa 2'-5'-oligoadenylate synthase-like protein isoform b
<i>HLA-A</i>	1.23	2.51E-11	4.39617E-10	HLA class I histocompatibility antigen, A-1 alpha chain precursor

cantly increased in Prdx6-interference HEECs. IL-6 is required for the activation of the JAK-STAT pathway in myocardial infarction [37], in myeloma [38], head and neck tumors [39], and primary breast cancer [40]. These reports are consistent with our findings, which indicated the activation of IL-6/JAK1/STAT1 signaling axis in Prdx6-interference HEECs.

IFN γ is one of the most important cytokines and plays an important role in defenses against microbial infections by producing various cytokines and inducing autophagy [41]. The activation of the JAK2/STAT1 signaling pathway by IFN γ has been reported in Epstein-Barr virus-positive gastric cancer [42]. In the present study, although we did not observe significant differences in expression levels of IFN γ and

IFN γ receptor between Prdx6-interference and control HEECs, the expression levels of eighteen IFN-related genes were significantly increased, as well as the expression levels of downstream targets (*OAS1*, *OAS2*, *OAS3*, *OASL*, *HLA-A*) of IFN γ signaling in Prdx6-interference HEECs. We believe that the expression levels of IFN γ and IFN γ receptor were transiently increased after *Prdx6* knockdown but returned to normal levels when we performed our measurements. Additional time course studies need to be performed to determine if IFN γ and IFN γ receptor expression levels are transiently increased after Prdx6 knockdown.

In conclusion, we demonstrated that knockdown of Prdx6 induced higher levels of ROS in HEECs, which

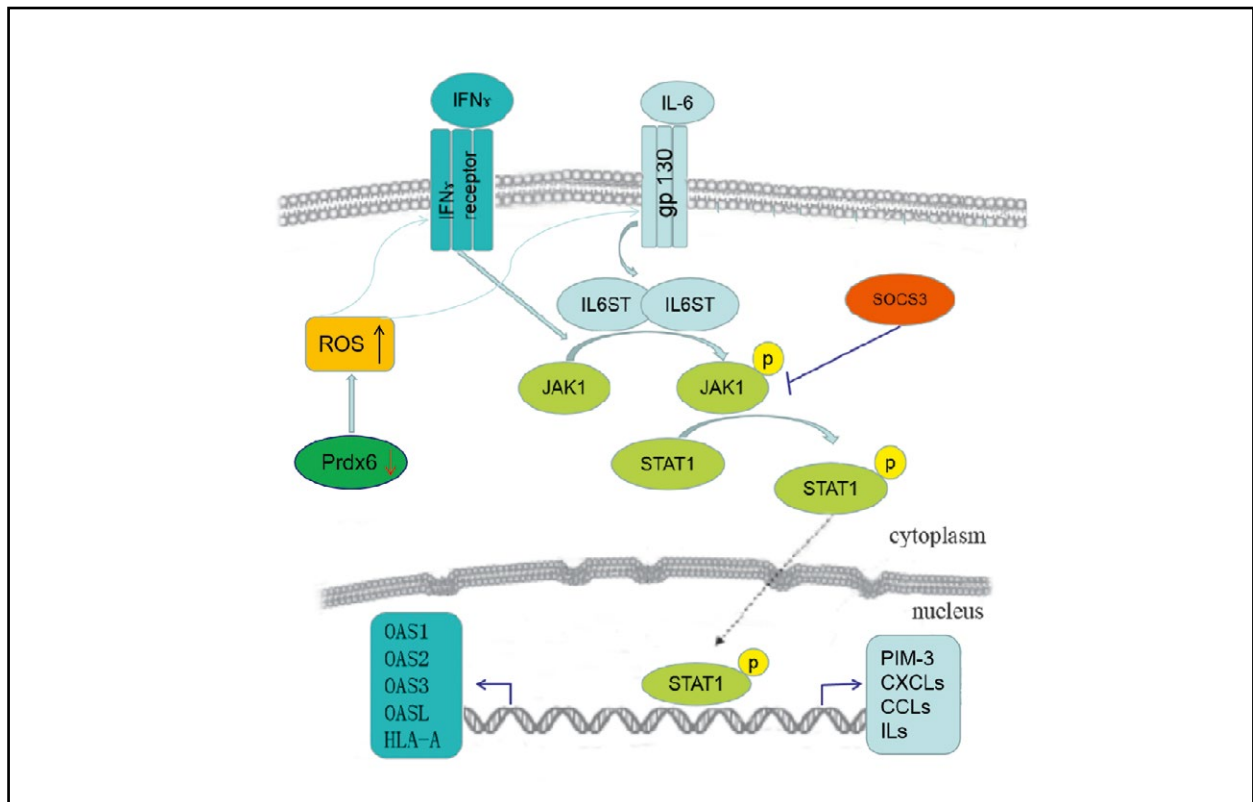


Figure 6. The likely JAK1/STAT1 signaling pathway's associations with Prdx6 expression in HECCs. The knockdown of Prdx6 induced the higher levels of ROS in HECCs, which in turn, activated the *IL-6* receptor and *IFN γ* to induce the JAK1/STAT1 signaling pathway. Meanwhile, the inhibitor of JAK1/STAT1 signaling pathway, SOCS3, was significantly reduced in Prdx6-interference HECCs. Both *IL-6* receptor and *IFN γ* might promote the phosphorylation of JAK1. Then, the phosphorylated JAK1 promoted the phosphorylation of STAT1. The phosphorylated STAT1 was transferred into the nucleus, and activated the expressions of a series of effector genes.

in turn, activated the *IL-6* receptor and *IFN γ* to induce the JAK1/STAT1 signaling pathway.

Funding

This work was supported by a grant from the National Key R&D Program of China (Grant No. 2018YFC1003600).

References

- Jin DY, Chae HZ, Rhee SG, et al. Regulatory role for a novel human thioredoxin peroxidase in NF-kappaB activation. *J Biol Chem.* 1997; 272(49): 30952–30961, doi: 10.1074/jbc.272.49.30952, indexed in Pubmed: 9388242.
- Chowdhury I, Mo Y, Gao L, et al. Oxidant stress stimulates expression of the human peroxiredoxin 6 gene by a transcriptional mechanism involving an antioxidant response element. *Free Radic Biol Med.* 2009; 46(2): 146–153, doi: 10.1016/j.freeradbiomed.2008.09.027, indexed in Pubmed: 18973804.
- Ray PD, Huang BW, Tsuji Y. Reactive oxygen species (ROS) homeostasis and redox regulation in cellular signaling. *Cell Signal.* 2012; 24(5): 981–990, doi: 10.1016/j.cellsig.2012.01.008, indexed in Pubmed: 22286106.
- O'Leary PC, Terrile M, Bajor M, et al. Peroxiredoxin-1 protects estrogen receptor α from oxidative stress-induced suppression and is a protein biomarker of favorable prognosis in breast cancer. *Breast Cancer Res.* 2014; 16(4): R79, doi: 10.1186/bcr3691, indexed in Pubmed: 25011585.
- Li XJ, Xu M, Zhao XQ, et al. Proteomic analysis of synovial fibroblast-like synoviocytes from rheumatoid arthritis. *Clin Exp Rheumatol.* 2013; 31(4): 552–558, indexed in Pubmed: 23739258.
- Moon EY, Noh YW, Han YH, et al. T lymphocytes and dendritic cells are activated by the deletion of peroxiredoxin II (Prx II) gene. *Immunol Lett.* 2006; 102(2): 184–190, doi: 10.1016/j.imlet.2005.09.003, indexed in Pubmed: 16290204.
- Szabó-Taylor KÉ, Eggleton P, Turner CAL, et al. Lymphocytes from rheumatoid arthritis patients have elevated levels of intracellular peroxiredoxin 2, and a greater frequency of cells with exofacial peroxiredoxin 2, compared with healthy human lymphocytes. *Int J Biochem Cell Biol.* 2012; 44(8): 1223–1231, doi: 10.1016/j.biocel.2012.04.016, indexed in Pubmed: 22565169.
- Huh JY, Kim Y, Jeong J, et al. Peroxiredoxin 3 is a key molecule regulating adipocyte oxidative stress, mitochondrial biogenesis, and adipokine expression. *Antioxid Redox Signal.* 2012; 16(3): 229–243, doi: 10.1089/ars.2010.3766, indexed in Pubmed: 21902452.
- Guo X, Yamada S, Tanimoto A, et al. Overexpression of peroxiredoxin 4 attenuates atherosclerosis in apolipoprotein E knockout mice. *Antioxid Redox Signal.* 2012; 17(10): 1362–1375, doi: 10.1089/ars.2012.4549, indexed in Pubmed: 22548251.

10. Schulte J. Peroxiredoxin 4: a multifunctional biomarker worthy of further exploration. *BMC Med.* 2011; 9: 137, doi: 10.1186/1741-7015-9-137, indexed in Pubmed: 22196027.
11. Chang X, Cui Y, Zong M, et al. Identification of proteins with increased expression in rheumatoid arthritis synovial tissues. *J Rheumatol.* 2009; 36(5): 872–880, doi: 10.3899/jrheum.080939, indexed in Pubmed: 19369474.
12. Kropotov A, Usmanova N, Serikov V, et al. Mitochondrial targeting of human peroxiredoxin V protein and regulation of PRDX5 gene expression by nuclear transcription factors controlling biogenesis of mitochondria. *FEBS J.* 2007; 274(22): 5804–5814, doi: 10.1111/j.1742-4658.2007.06103.x, indexed in Pubmed: 17937766.
13. Park MiH, Jo M, Kim YuRi, et al. Roles of peroxiredoxins in cancer, neurodegenerative diseases and inflammatory diseases. *Pharmacol Ther.* 2016; 163: 1–23, doi: 10.1016/j.pharmthera.2016.03.018, indexed in Pubmed: 27130805.
14. Yun HM, Choi DY, Oh KiW, et al. PRDX6 exacerbates dopaminergic neurodegeneration in a MPTP mouse model of parkinson's disease. *Mol Neurobiol.* 2015; 52(1): 422–431, doi: 10.1007/s12035-014-8885-4, indexed in Pubmed: 25193021.
15. Yun HM, Park KR, Kim EC, et al. PRDX6 controls multiple sclerosis by suppressing inflammation and blood brain barrier disruption. *Oncotarget.* 2015; 6(25): 20875–20884, doi: 10.18632/oncotarget.5205, indexed in Pubmed: 26327204.
16. Yun HM, Park KR, Park MiH, et al. PRDX6 promotes tumor development via the JAK2/STAT3 pathway in a urethane-induced lung tumor model. *Free Radic Biol Med.* 2015; 80: 136–144, doi: 10.1016/j.freeradbiomed.2014.12.022, indexed in Pubmed: 25582888.
17. Kim DH, Lee DH, Jo MiR, et al. Exacerbation of collagen antibody-induced arthritis in transgenic mice overexpressing peroxiredoxin 6. *Arthritis Rheumatol.* 2015; 67(11): 3058–3069, doi: 10.1002/art.39284, indexed in Pubmed: 26211509.
18. O'Shea JJ, Gadina M, Schreiber RD. Cytokine signaling in 2002: new surprises in the Jak/Stat pathway. *Cell.* 2002; 109 Suppl: S121–S131, doi: 10.1016/s0092-8674(02)00701-8, indexed in Pubmed: 11983158.
19. Herrera SC, Bach EA. JAK/STAT signaling in stem cells and regeneration: from vertebrates. *Development.* 2019; 146(2), doi: 10.1242/dev.167643, indexed in Pubmed: 30696713.
20. Baker BJ, Akhtar LN, Benveniste EN. SOCS1 and SOCS3 in the control of CNS immunity. *Trends Immunol.* 2009; 30(8): 392–400, doi: 10.1016/j.it.2009.07.001, indexed in Pubmed: 19643666.
21. Alston CI, Dix RD. SOCS and herpesviruses, with emphasis on cytomegalovirus retinitis. *Front Immunol.* 2019; 10: 732, doi: 10.3389/fimmu.2019.00732, indexed in Pubmed: 31031749.
22. Fernandez MC, O'Flaherty C. Peroxiredoxin 6 is the primary antioxidant enzyme for the maintenance of viability and DNA integrity in human spermatozoa. *Hum Reprod.* 2018; 33(8): 1394–1407, doi: 10.1093/humrep/dey221, indexed in Pubmed: 29912414.
23. Shi H, Liu J, Zhu P, et al. Expression of peroxiredoxins in the human testis, epididymis and spermatozoa and their role in preventing H2O2-induced damage to spermatozoa. *Folia Histochem Cytobiol.* 2018; 56(3): 141–150, doi: 10.5603/FHC.a2018.0019, indexed in Pubmed: 30187908.
24. Zhou W, De Iulius GN, Dun MD, et al. Characteristics of the Epididymal Luminal Environment Responsible for Sperm Maturation and Storage. *Front Endocrinol (Lausanne).* 2018; 9: 59, doi: 10.3389/fendo.2018.00059, indexed in Pubmed: 29541061.
25. Dubé E, Dufresne J, Chan PTK, et al. Assessing the role of claudins in maintaining the integrity of epididymal tight junctions using novel human epididymal cell lines. *Biol Reprod.* 2010; 82(6): 1119–1128, doi: 10.1095/biolreprod.109.083196, indexed in Pubmed: 20164436.
26. Holen T, Amarzguoui M, Wiiger MT, et al. Positional effects of short interfering RNAs targeting the human coagulation trigger tissue factor. *Nucleic Acids Res.* 2002; 30(8): 1757–1766, doi: 10.1093/nar/30.8.1757, indexed in Pubmed: 11937629.
27. 't Hoen PAC, Ariyurek Y, Thygesen HH, et al. Deep sequencing-based expression analysis shows major advances in robustness, resolution and inter-lab portability over five microarray platforms. *Nucleic Acids Res.* 2008; 36(21): e141, doi: 10.1093/nar/gkn705, indexed in Pubmed: 18927111.
28. Morrissey AS, Morin RD, Delaney A, et al. Next-generation tag sequencing for cancer gene expression profiling. *Genome Res.* 2009; 19(10): 1825–1835, doi: 10.1101/gr.094482.109, indexed in Pubmed: 19541910.
29. Audic S, Claverie JM. The significance of digital gene expression profiles. *Genome Res.* 1997; 7(10): 986–995, doi: 10.1101/gr.7.10.986, indexed in Pubmed: 9331369.
30. Benjamini Y, Yekutieli D, et al. The control of the false discovery rate in multiple testing under dependency. *Ann. Statist.* 2001; 29(4): 1165–1188, doi: 10.1214/aos/1013699998.
31. Ye J, Fang L, Zheng H, et al. WEGO: a web tool for plotting GO annotations. *Nucleic Acids Res.* 2006; 34(Web Server issue): W293–W297, doi: 10.1093/nar/gkl031, indexed in Pubmed: 16845012.
32. Kanehisa M, Araki M, Goto S, et al. KEGG for linking genomes to life and the environment. *Nucleic Acids Res.* 2008; 36(Database issue): D480–D484, doi: 10.1093/nar/gkm882, indexed in Pubmed: 18077471.
33. Leong KP, Tee NW, Yap WM, et al. Nocardiosis in patients with systemic lupus erythematosus. The Singapore Lupus Study Group. *J Rheumatol.* 2000; 27(5): 1306–1312, indexed in Pubmed: 10813308.
34. Amoyel M, Anderson AM, Bach EA. JAK/STAT pathway dysregulation in tumors: a Drosophila perspective. *Semin Cell Dev Biol.* 2014; 28: 96–103, doi: 10.1016/j.semcdb.2014.03.023, indexed in Pubmed: 24685611.
35. Kleppe M, Spitzer MH, Li S, et al. Jak1 integrates cytokine sensing to regulate hematopoietic stem cell function and stress hematopoiesis. *Cell Stem Cell.* 2017; 21(4): 489–501.e7, doi: 10.1016/j.stem.2017.08.011, indexed in Pubmed: 28965767.
36. Zhao XF, Wan J, Powell C, et al. Leptin and IL-6 family cytokines synergize to stimulate Müller glia reprogramming and retina regeneration. *Cell Rep.* 2014; 9(1): 272–284, doi: 10.1016/j.celrep.2014.08.047, indexed in Pubmed: 25263554.
37. Dawn B, Xuan YT, Guo Y, et al. IL-6 plays an obligatory role in late preconditioning via JAK-STAT signaling and upregulation of iNOS and COX-2. *Cardiovasc Res.* 2004; 64(1): 61–71, doi: 10.1016/j.cardiores.2004.05.011, indexed in Pubmed: 15364614.
38. Puthier D, Bataille R, Amiot M. IL-6 up-regulates mcl-1 in human myeloma cells through JAK/STAT rather than ras/MAP kinase pathway. *Eur J Immunol.* 1999; 29(12): 3945–3950, doi: 10.1002/(sici)1521-4141(199912)29:12<3945::aid-immu3945>3.0.co;2-o, indexed in Pubmed: 10602002.
39. Yadav A, Kumar B, Datta J, et al. IL-6 promotes head and neck tumor metastasis by inducing epithelial-mesenchymal transition via the JAK-STAT3-SNAIL signaling pathway. *Mol Cancer Res.* 2011; 9(12): 1658–1667, doi: 10.1158/1541-7786.MCR-11-0271, indexed in Pubmed: 21976712.
40. Chang Q, Bournazou E, Sansone P, et al. The IL-6/JAK/Stat3 feed-forward loop drives tumorigenesis and metastasis. *Neoplasia.* 2013; 15(7): 848–862, doi: 10.1593/neo.13706, indexed in Pubmed: 23814496.

41. Yamamoto M, Okuyama M, Ma JiSu, et al. A cluster of interferon- γ -inducible p65 GTPases plays a critical role in host defense against *Toxoplasma gondii*. *Immunity*. 2012; 37(2): 302–313, doi: 10.1016/j.immuni.2012.06.009, indexed in Pubmed: 22795875.
42. Moon JiW, Kong SK, Kim BS, et al. IFN γ induces PD-L1 overexpression by JAK2/STAT1/IRF-1 signaling in EBV-positive gastric carcinoma. *Sci Rep*. 2017; 7(1): 17810, doi: 10.1038/s41598-017-18132-0, indexed in Pubmed: 29259270.

Submitted: 22 January, 2022

Accepted after reviews: 19 July, 2022

Available as AoP: 4 August, 2022